Phase-field Modeling of Eutectic Solidification: From Oscillations to Invasion

Roger Folch* and Mathis Plapp
Laboratoire de Physique de la Matière Condensée, CNRS/École Polytechnique, 91128 Palaiseau, France
* *e-mail addresses: rf@pmc.polytechnique.fr, roger@gps.jussieu.fr, roger@ecm.ub.es*

Abstract

We develop a phase-field model of eutectic growth that uses three phase fields, admits strictly binary interfaces as stable solutions, and has a smooth free energy functional. We use this model to simulate oscillatory limit cycles in two-dimensional lamellar growth, and find a continuous evolution from low-amplitude oscillations to successive invasions of one solid phase by the other when the lamellar spacing is varied.

I. INTRODUCTION

Solidification is both a fascinating example of pattern formation out of equilibrium and a phenomenon of practical importance in metallurgy. The most common solidification microstructures found in industrial alloys are dendrites and eutectic composite structures (rods or lamellae). Eutectic growth occurs when two solid phases of different composition can solidify from the same melt. The interplay between the redistribution of chemical components in front of the moving phase boundary and the effects of capillarity along the curved interfaces gives rise to a wealth of different patterns and nonlinear phenomena such as bifurcations, limit cycles, solitary waves, and even chaotic states [1].

Phase-field modeling has become the method of choice for simulating solidification fronts. Its main advantage is that it avoids explicit tracking of the solidification front by introducing "phase fields" that vary continuously between constant values corresponding to the bulk phases, thus replacing the sharp fronts by diffuse interfaces with a finite thickness. The connection to the traditional free-boundary formulation of solidification is established by the technique of matched asymptotic expansions around the equilibrium front in the limit where the thickness of the diffuse interfaces is much smaller than all other relevant length scales. Recently, the computational efficiency of phase-field models for single-phase solidification of pure substances and binary alloys has been drastically enhanced by pushing this perturbation analysis to second order [2]. This, combined with a random walk algorithm for an efficient simulation of the diffusion equation, has made it possible to simulate quantitatively the dendritic growth of a pure substance in three dimensions for experimentally relevant parameters [3].

Therefore, it would be highly desirable to extend this second-order asymptotic analysis to phase-field models for multi-phase solidification; we will specifically address the case of

eutectic growth, where two solid phases denoted by α and β grow from the liquid. The first phase-field models for eutectic growth used the standard phase field to distinguish between solid and liquid, and a concentration field [4,5] or a second phase field [6] to distinguish between the two solids. However, a solid-liquid interface then involves variations of the two variables and the asymptotic analysis becomes extremely cumbersome. The more recent multi-phase-field approach [7] assigns one phase field to each phase and interprets these fields as local volume fractions. Across an interface, in principle only the volume fractions of the two bulk phases limiting the interface need to vary, and one of them can be eliminated in terms of the other. Hence, this method allows for equilibrium interface solutions depending on a single variable that are equivalent to the usual "binary" interfaces of the standard phase-field model. However, to achieve this the model has to be carefully designed, and so far strictly binary interfaces have only been obtained by using a singular free energy (double obstacle potential) [8], which might complicate the asymptotic analysis.

We present a phase-field model for eutectic growth that uses three phase fields, yields exactly binary interfaces at equilibrium, and has a smooth free energy functional. Furthermore, the free energy is designed to keep the interfaces binary to first order in the usual non-equilibrium asymptotic expansion, which makes it a promising starting point for a second-order analysis.

To illustrate the capabilities of the model in its present form, we simulate lamellar eutectic growth of a simple model alloy with a symmetric phase diagram. We show that small-amplitude oscillations of the lamellar width, "giant oscillations", and successive invasions of one solid phase by the other, each of which is seen in experiments, all belong to the same branch of oscillatory limit cycles that is parametrized by the lamellar spacing.

II. MODEL

We use three phase fields $p_i \in [0,1]$ representing the local volume fractions of each phase (α, β or liquid), and thus $\sum_i p_i = 1$. Their dynamics is derived from a free energy functional $\mathcal{F}$,

$$\frac{\partial p_i}{\partial t} = -\frac{1}{\tau}\frac{\delta \mathcal{F}}{\delta p_i} \quad , \tag{1}$$

where τ is a relaxation time and the variational derivative has to take into account the constraint $\sum_i p_i = 1$. Furthermore, the concentration field c obeys the conserved dynamics

$$\partial c/\partial t = \vec{\nabla}\left[M(p_\alpha, p_\beta, p_l)\vec{\nabla}\mu\right] \quad , \tag{2}$$

where $\mu \equiv \delta\mathcal{F}/\delta c$ is the chemical potential and M is a phase-dependent mobility.

The free energy functional $\mathcal{F} = \int_V f dV$ is the volume integral of a free energy density f that is conveniently decomposed into $f = f_{\rm grad} + f_{\rm TW} + f_c$, where $f_{\rm TW}$ is a triple well potential with minima on each pure phase — the equivalent of the double well potential of the standard phase-field model, $f_{\rm grad}$ contains the gradients of the phase fields and ensures a finite interface thickness and surface tension, and f_c couples the phase fields and the concentration and drives the system out of equilibrium.

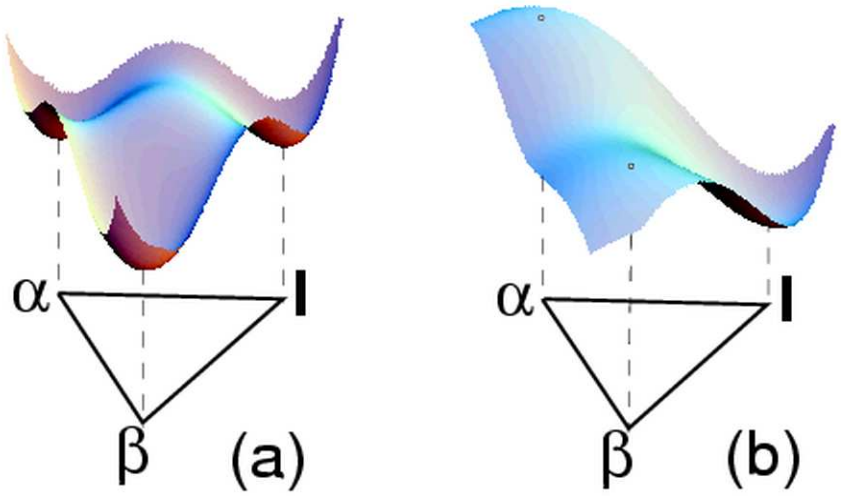

FIG. 1. Triple-well potential f_{TW} (a) and elementary tilt function $-g_l$ (b) drawn as "landscapes" over the Gibbs simplex.

Due to the constraint $\sum_i p_i = 1$, the free energy density and the interface solutions can be conveniently represented on a *Gibbs simplex*, that is an equilateral triangle where the distance to each side of the triangle from a given point represents the value of one of the phase fields. Thus, each vertex corresponds to a pure phase, and each side to a purely binary interface. Our goal is to obtain strictly binary interfaces, i.e., the equilibrium solutions of (1) for an interface connecting two phases should exactly run along the edges of the simplex. One way to achieve this is to choose

$$f_{\rm grad} = \frac{W^2}{2} \sum_i |\vec{\nabla} p_i|^2 \ , \tag{3}$$

and to design the function f_{TW} in such a way that the three minima are connected by "saddles" that run along the edges and that have vanishing derivatives in the direction normal to the edges. Such functions can be constructed using the geometry of the Gibbs simplex, as will be detailed elsewhere. The simplest choice,

$$f_{\rm TW} = \sum_i p_i^2 (1 - p_i)^2 \ , \tag{4}$$

is plotted in Fig. 1a and reduces to the standard fourth-degree double well potential of the binary phase-field model on the edges. With these choices, the free energy is completely symmetric with respect to the interchange of any two phases, and as a consequence all three surface tensions are equal. However, the general case of unequal surface tensions can also be treated by adding other terms in the free energy density that modify the height of the saddle points.

Out of equilibrium, the triple well is "tilted" by the term f_c in order to favor one phase over the others. Since we want to keep the interfaces binary, this term needs to be carefully constructed. The elementary building blocks are tilt functions g_i that satisfy $g_i = 1$ for $p_i = 1$, $g_i = 0$ for $p_j = 1$, $j \neq i$, and that have vanishing derivatives in the direction normal to the edges of the simplex. One possible choice is

$$g_i = 1 - \Big[(1+p_j-p_i)^2(2+p_i-p_j)^2 + (1+p_k-p_i)^2(2+p_i-p_k)^2 + (p_k-p_j)^2(3-|p_k-p_j|)^2\Big]/12 \ . \quad (5)$$

In Fig. 1b, we plot $-g_l$ that lowers the well for the liquid with respect to the two others. With the help of these functions,

$$f_c = \frac{1}{2}\left[c - \sum_i A_i g_i\right]^2 + \sum_i B_i g_i \quad (6)$$

interpolates between the concentration-dependent free energies $f_i = (c-A_i)^2/2 + B_i$ of each phase i. Here, $c = (C - C_E)/\Delta C$ is a scaled concentration variable, where $\Delta C = C_\beta - C_\alpha$ is the width of the eutectic plateau, and C_α, C_β, and C_E are the equilibrium compositions of the two solids and the liquid at the eutectic temperature. An arbitrary phase diagram can be constructed by performing the well-known double tangent construction, which yields $c_i^{ij} = A_i + (B_j - B_i)/(A_j - A_i)$ for the equilibrium concentration c_i^{ij} of phase i coexisting with phase j, and by choosing appropriate $A_i(T)$, $B_i(T)$, where T is the temperature. Note that by the same procedure, a peritectic phase diagram can be constructed [9].

Finally, we need to specify the mobility function in (2). Since $\partial^2 f_i/\partial c^2 \equiv 1$, the choice $M(p_\alpha, p_\beta, p_l) = Dp_l$ yields a constant diffusivity D in the liquid, and no diffusion in the solid (one-sided model).

III. SIMULATIONS

In thin-sample directional solidification of eutectic alloys with global composition in the eutectic range, the basic pattern is a periodic array of alternating lamellae of each solid phase, growing perpendicular to the large-scale solidification front and parallel to the imposed temperature gradient. This basic state exhibits various instabilities that have been carefully studied both experimentally in the transparent organic alloy CBr_4-C_2Cl_6 [1] and by numerical simulations using the boundary integral method [10]. For fixed experimental parameters, the stability of the basic state is controlled by the width of one lamella pair, or *lamellar spacing*. For sample compositions close to the eutectic point, the first instability that is encountered for increasing spacing is a period-preserving oscillatory instability, that is, the lamellae start to oscillate, with all the lamellae of the same phase oscillating in phase, and the global spacing left unchanged. Beyond the onset of this instability, stable limit cycles are found, with an oscillation amplitude that increases with spacing. In the boundary integral simulations, this branch of solutions terminates when the amplitude becomes too large because the thinner lamellae pinch off. In contrast, in experiments "giant oscillations" with very large amplitudes can be obtained [11]. Furthermore, when the experiments are started from a single solid phase growing into the liquid with a few widely spaced nuclei of the other solid phase on the solidification front, the nuclei grow and spread along the front forming "invasion tongues" [12]. When two tongues growing in opposite directions collide, they do not coalesce; instead, a narrow channel of the other phase remains and the whole process starts over with the role of the two phases reversed. The interface dynamics is hence still oscillatory, even if the patterns look completely different. In this regime, the boundary integral method becomes inapplicable because it uses the quasistationary approximation of

the diffusion equation that is valid only if the interface motion is slow compared to the diffusive solute redistribution. Here, we investigate oscillatory limit cycles with our phase-field model, that does not have this restriction.

The sample is solidified with pulling speed V in a constant temperature gradient G directed along the z direction. For simplicity, we use a symmetric phase diagram that has constant concentration jumps across the interfaces (parallel liquidus and solidus lines). This is implemented by choosing $A_\alpha = -0.5$, $A_\beta = 0.5$, $A_l = 0$, $B_\alpha = B_\beta = 0$ and $B_l = -(z - Vt)/l_T$, where $l_T = (m\Delta C)/G$ is the thermal length, with m being the liquidus slope (equal for both phases). The other relevant physical length scales are the diffusion length $l_D = D/V$ and the capillary length $d_0 = \Gamma/(m\Delta C)$, where Γ is the Gibbs-Thomson constant. In terms of the model parameters, $d_0 = (2\sqrt{2}/3)W$. All simulations discussed here were performed with $\tau = W = D = 1$, $l_T/d_0 = 530$, $l_D/d_0 = 212$ and at exactly eutectic composition (that is, $c = 0$ far ahead of the front).

The equations are integrated by a standard explicit finite-difference scheme on a regular grid of spacing $0.8\ W$ for which we have checked that the discretization has converged. Since the diffusivity vanishes in the solid, the diffusion equation only needs to be solved in interfacial and liquid regions. Moreover, far ahead of the solidification front, it is solved using a variant of the random walker algorithm of Ref. [3] that will be detailed elsewhere. Two types of initial conditions are used. To obtain lamellar steady states, simulations are started from two flat lamellae in contact with the liquid. If the lamellar state is unstable, the numerical noise generated by the random walkers triggers the instability. Alternatively, simulations are started from a flat single solid phase at equilibrium with the liquid. Upon pulling, the interface recoils towards colder temperatures as a diffusion layer of the rejected component is gradually formed. When the undercooling reaches a predetermined value, nucleation is mimicked by placing a large enough semicircular nucleus of the other phase on top of the interface.

We restrict our attention here to period-preserving oscillations without lateral drift. Therefore, it is sufficient to simulate two adjacent half lamellae or half a nucleus of one solid phase on top of the other with reflecting (no-flux) boundary conditions on the sides of the simulation box that are parallel to the lamellae. The lamellar spacing λ is varied by changing the lateral size of the simulation box. In the figures below, for clarity we have reconstructed a whole lamella pair by reflecting the system with respect to one side of the box.

We start by constructing the branch of stable lamellar steady-state solutions and find the minimal undercooling spacing at $\lambda_{\min} \approx 85 d_0$, in good agreement with the prediction of the Jackson-Hunt theory [13], $\lambda_{\min} \approx 79 d_0$. Next, we start from a single nucleus and monitor the dynamics for increasing spacings. We find a bifurcation toward oscillatory limit cycles for λ close to $2\lambda_{\min}$. As shown in Fig. 2a, for $\lambda = 2\lambda_{\min}$ the oscillation already has an amplitude of about a quarter of the lamellar spacing, but its shape is still close to a sinusoidal wave. At $\lambda = 4\lambda_{\min}$ (Fig.2 2b), the oscillation is highly asymmetric, and has an amplitude close to half the lamellar spacing, i.e., only a thin channel of the other solid phase is left. Finally, at $8.48\lambda_{\min}$ (Fig. 2c), three different regimes become apparent: (i) initially, the nucleus grows slowly and spreads along the interface to form an invading finger with a well-defined shape, (ii) the finger speeds up with an approximately constant acceleration, leaving a straight border with the other solid phase behind, and (iii) when it approaches a

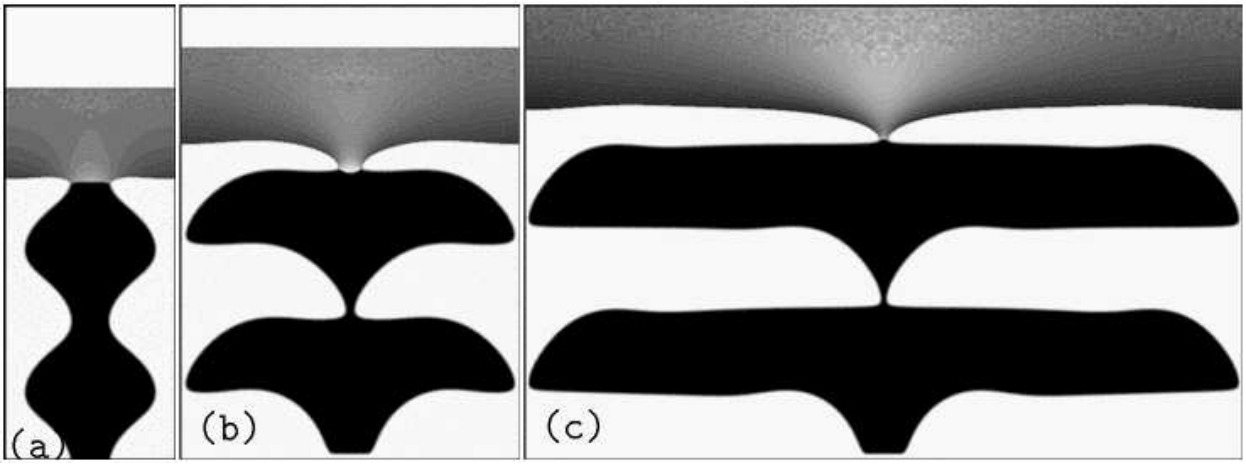

FIG. 2. Snapshot pictures of typical oscillatory structures. Growth is upwards, the two solids are black and white, and the greyscale in the liquid is proportional to the solute concentration. (a) low-amplitude oscillations ($\lambda/\lambda_{\min} = 2$), (b) giant oscillations ($\lambda/\lambda_{\min} = 4$), (c) successive invasions ($\lambda/\lambda_{\min} = 8.48$). The scale is the same on all three figures.

finger growing in the opposite direction (in our simulations, its mirror image generated by the reflecting boundary conditions), it "feels" the diffusion field generated by the other and slows down very rapidly, allowing for the other phase to emerge through a narrow channel left between the two fingers and thus restart the process with the role of the two solids reversed.

Remarkably, our largest simulations reproduce many characteristic features of the "successive invasions" observed in the experiments [12], in particular the approximately constant acceleration of invasion tongues and the leftover of narrow channels between "colliding" fingers. From our simulations, it hence appears that this regime can be understood as period-preserving oscillations with very large amplitudes. Indeed, the morphology at $4\lambda_{\min}$ already presents stages (i) and (iii), but not (ii). Apparently, to observe this intermediate, constant acceleration regime, it is sufficient to have enough "free space" left in front of the propagating finger (i.e., large lamellar spacings). It is also interesting to note that in peritectic alloys, simulations of spreading in the same geometry produce stages (i) and (ii), but then colliding fingers coalesce, and to obtain an oscillatory dynamics explicit nucleation events have to be introduced [9,14].

The fact that we can switch from gentle oscillations to long invading fingers just by changing the lamellar spacing demonstrates that both belong to the same branch of oscillatory limit cycles. This branch of solutions is indeed an attractor, since simulations at fixed spacing and started from very different initial conditions always converge to the same cycle.

IV. CONCLUSION

We have developed a phase-field model of eutectic solidification that has a smooth free energy landscape and yields exactly binary interfaces away from the trijunction points. These properties make it a promising starting point for a second-order asymptotic analysis. Furthermore, we have used the model to simulate oscillatory limit cycles in a model alloy

that has a symmetric phase diagram, and we have found that low-amplitude oscillations, "giant oscillations", and successive invasions, all observed in experiments, lie on a single branch of solutions that is parametrized by the lamellar spacing and that bifurcates from the steady-state branch at about twice the minimum undercooling spacing.

Here, we have focused on period-preserving oscillatory modes; many other instability modes exist, for example the tilt instability or period-doubling oscillations. These instabilities can be studied using less restrictive boundary conditions. Preliminary simulations show that for the case studied here, namely an alloy with symmetric phase diagram at its eutectic composition, period-preserving oscillations remain the only stable limit cycles. In contrast, if we use off-eutectic sample compositions or an asymmetric phase diagram, and hence break the complete symmetry between the two solid phases, other modes become active. Therefore, our model can be used to obtain a more complete bifurcation diagram, which is the subject of ongoing work.

We thank Silvère Akamatsu and Gabriel Faivre for many stimulating discussions and Jean-François Gouyet for his help with Fig. 1. R. F. acknowledges financial support from project FMRX-CT96-0085 of the European Commission and from Centre National d'Études Spatiales (France).

REFERENCES

[1] Ginibre, M., Akamatsu, S., Faivre, G.: Experimental determination of the stability diagram of a lamellar eutectic growth front. Phys. Rev. E **56** (1997) 780–796

[2] Karma, A., Rappel, W.-J.: Quantitative phase-field modeling of dendritic growth in two and three dimensions. Phys. Rev. E **57** (1998) 4323–4349; Karma, A.: Phase-Field Formulation for Quantitative Modeling of Alloy Solidification. Phys. Rev. Lett. **87** (2001) 115701

[3] Plapp, M., Karma, A.: Multiscale random-walk algorithm for simulating interfacial pattern formation. Phys. Rev. Lett. **84** (2000) 1740–1743; Plapp, M., Karma, A.: Multiscale Finite-Difference-Diffusion-Monte-Carlo method for simulating dendritic solidification. J. Comp. Phys. **165** (2000) 592–619

[4] Karma, A.: Phase-field model of eutectic growth. Phys. Rev. E **49** (1994) 2245–2250

[5] Elder, K. R., Drolet, F., Kosterlitz, J. M., Grant, M.: Stochastic eutectic growth. Phys. Rev. Lett. **72** (1994) 677–680

[6] Wheeler, A. A., McFadden, G. B., Boettinger, W. J.: Phase-field model for solidification of a eutectic alloy. Proc. R. Soc. Lond. A **452** (1996) 495–525

[7] Steinbach, I., Pezzola, F., Nestler, B., Seeßelberg, M., Prieler, R., Schmitz, G. J.: A phase field concept for multiphase systems. Physica D **94** (1996) 135–147

[8] Garcke, H., Nestler, B., Stoth, B.: A multi phase field concept: numerical simulations of moving phase boundaries and multiple junctions. SIAM J. Appl. Math **60** (1999) 295–315

[9] Lo, T. S., Karma, A., Plapp, M.: Phase-field modeling of microstructural pattern formation during directional solidification of peritectic alloys without morphological instability. Phys. Rev. E **63** (2001) 031504

[10] Karma, A., Sarkissian, A.: Morphological instabilities of lamellar eutectics. Metall. Mater. Trans **27A** (1996) 635–656

[11] Akamatsu, S., Faivre, G.: Private communication.

[12] Akamatsu, S., Moulinet, S., Faivre, G.: The Formation of Lamellar-Eutectic Grains in Thin Samples. Metall. Mater. Trans. **32A** (2001) 2039–2047

[13] Jackson, K. A., Hunt, J. D.: Lamellar and rod eutectic growth. Trans. Metall. Soc. AIME **236** (1966) 843–852

[14] Nestler, B., Wheeler, A. A.: A multi-phase-field model of eutectic and peritectic alloys: numerical simulation of growth structures. Physica D **138** (2000) 114–133